International Journal for Housing Science and Its Applications
Publish August 10, 2025. Volume 46, Issue 4 Pages 8109-8121

https://doi.org/10.70517/ijhsa464694

A Case Study on the Hydrological Effects of Smart Technology on Urban Rainwater Gardens

Jie Tian[1] and Dongdong Gao[2,*]
[1] Fine Arts & Design College, Minjiang University, Fuzhou, Fujian, 350108, China
[2] School of Urban Construction, Fuzhou Technology and Business University, Fuzhou, Fujian, 350108, China
Corresponding authors: (e-mail: 2160@mju.edu.cn).

Abstract: This study uses a rain garden in a certain city as a case study and analyzes its hydrological effects based on the SWMM model. A comparative analysis was conducted between drainage-type (RG-dr) and infiltration-type (RG-inf) rain gardens to explore the impact of different design types of rain gardens on runoff regulation, pollutant reduction, and landscape benefits. The average total pollutant load for the four categories in RG-dr was 56.383 kg, 13.725 kg, 7.484 kg, and 0.904 kg, respectively. The average removal rates for the four categories of pollutants (SS, COD, TN, and TP) were 29.30%, 33.15%, 31.52%, and 39.08%, respectively. Most users considered the landscape effects of RG-dr to be good, with over 50% of users across all age groups rating them as “very good” or “good.” Users generally believed that RG-dr had rich landscape layers, with over 60% of users across all age groups rating them as “very rich” or “relatively rich.”

Index Terms rain garden, SWMM model, hydrological effects, runoff regulation, landscape benefits

I. Introduction

In recent years, urban flooding has become increasingly severe. This is because, in the process of accelerating urbanization, the increase in paved surfaces has significantly reduced the amount of rainwater infiltration, the reduction in green spaces has weakened the vegetation's ability to retain rainwater, and there are certain defects in the design of urban rainwater drainage systems, leading to surface water being unable to infiltrate [1]-[3]. At the same time, water scarcity and water pollution in cities are also extremely severe [4]. Furthermore, under urban development, vast areas of farmland and natural vegetation have been replaced by streets, factories, and residential buildings, resulting in significant changes in the surface's water retention, permeability, and thermal conditions. These changes affect the relationship between precipitation and runoff, weaken the natural storage capacity within the watershed, and consequently lead to corresponding changes in the hydrological elements and processes within urban areas and their suburbs [5]-[8]. Urban hydrological effects refer to the series of impacts that urban development has on hydrological processes [9]. Against this backdrop, the concept of “sponge cities” has been proposed, which refers to the ability of cities to absorb, store, and discharge water, thereby adapting to changes in the natural environment and climate [10]. In applying this concept, the most important principle is to follow natural laws.

Rain gardens are the basic units for implementing the sponge city concept, capable of collecting rainwater from road surfaces and rooftops with good storage capacity, thereby achieving the goal of rainwater recycling. Their construction costs are relatively low, and they must balance water management with the aesthetic and functional aspects of a garden [11]-[13]. Typically, rain gardens are small in size but resemble natural ecosystems the most. Through this approach, rainwater in urban areas can be treated and purified, and the purified water can be used for landscaping, truly achieving a three-in-one function of landscaping, rainwater collection, and purification [14]-[16]. Rain gardens are generally classified into two types: permeable and semi-storage/semi-permeable. The former provides an effective supply of surface water [17]. The latter requires integrating permeation and storage functions during construction, utilizing plants' ecological purification capabilities to ensure effluent meets relevant standards. Such rain gardens fully integrate rainwater purification functions, achieving purification and filtration objectives, thereby improving urban water quality [18]-[20]. Literature [21] indicates that rain garden layout not only enhances urban pollutant reduction rates but also increases stormwater runoff reduction rates, thereby mitigating flood disasters. Based on this, many researchers have begun to focus on the hydrological effects of rain gardens. Literature [22] developed a numerical model to calculate the effective area of rain gardens and established methods for assessing hydrological efficiency, thereby optimizing the application of rain gardens in drainage and water quality management. Literature [23] pointed out that rain garden design is closely related to its hydrological characteristics,

so a hydrological infiltration model was constructed. Simulation results showed that minimizing overflow risks during heavy rainfall events in rain gardens requires consideration of water column height.

In recent years, the application of intelligent technologies has expanded to include rain gardens. Reference [24] utilized the Zebra optimization algorithm to optimize the backpropagation neural network (BP), support vector machine, and random forest algorithms, thereby constructing a predictive model for rain garden runoff control effectiveness. The improved BP predictive model demonstrated the best performance. Literature [25] designed a deep learning model to predict the concentrations of total suspended solids, chemical oxygen demand, total nitrogen, and total phosphorus, as well as a water quality prediction model supported by a long short-term memory network, aiming to monitor the stormwater runoff characteristics of rain garden facilities and observe their pollutant removal and water volume reduction capabilities under hydrological changes. Literature [26] used the Phillips model, gradient boosting machine, and deep learning to conduct an in-depth study of infiltration rates under different vegetation types, plant densities, and water flow conditions in rain gardens, with the gradient boosting machine yielding the best prediction performance. Additionally, Reference [27] utilized 3D modeling technology and digital twin technology to visualize hydrological data in Hankou, Wuhan. By constructing a 3D scene, the study achieved data-scene interaction. Under advanced programming, it simulated flood seasonal evolution and other visualization functions to assist decision-making. Reference [28] introduced an outdoor multi-hop wireless sensor network capable of collecting hydrological environmental data, and used this to construct a networked sensor system for analyzing basin hydrological conditions.

This paper first introduces the definition and classification of rain gardens and systematically explains their design and construction methods. It provides a detailed explanation of the principles of SWMM from the perspectives of hydrology and hydraulics, and uses the dynamic wave method to simulate the water depth at nodes in the stormwater pipe network system and the movement of pressurized water flow within the pipes. By collecting basic data from the study area, a hydrological model of the study area is constructed. Taking RG-dr and RG-inf rain gardens as the research objects, the study quantifies the impact of different design types on runoff regulation, peak detention time, and pollutant load. By combining case data with user surveys, the study comprehensively evaluates the multi-dimensional benefits of rain gardens.

II. Research on the hydrological effects of urban rain gardens based on the SWMM model

II. A. Design and Construction of Rain Gardens

Against the backdrop of global climate change and accelerating urbanization, urban stormwater management faces severe challenges. As a core facility of low impact development (LID), optimizing the hydrological effects and environmental benefits of rain gardens has become a hot topic of research.

II. A. 1) Site Selection

Site selection is crucial for the construction of rain gardens. Proper utilization of terrain can reduce construction volume and lower costs. Site selection should follow the following principles:

(1) Rain gardens should be constructed in low-lying areas without long-term water accumulation or in areas where rainwater runoff can flow through;

(2) Rain gardens should be at least 4 meters away from buildings to avoid seepage affecting building foundations and causing safety hazards;

(3) Rain gardens are best located in areas that receive ample sunlight.

II. A. 2) Depth and slope

Rain gardens require a certain slope to collect rainwater, and drainage lines should be designed along the slope to effectively channel rainwater into the rain garden. An appropriate slope facilitates sufficient contact between rainwater, plants, and soil, thereby achieving the purpose of purification. The ground slope of a rain garden should be $\leqslant$15%, with a recommended depth of approximately 13 cm.

II. A. 3) Design Methods

Currently, three common methods are used for rain garden design, primarily including the infiltration method based on Darcy's law, the effective volume method of the storage layer, and the proportional estimation method based on the catchment area. The Darcy's Law-based infiltration method is designed based on the rain garden's own infiltration capacity and Darcy's Law, ignoring the water storage capacity of the rain garden's structural voids. The effective volume of the storage layer method primarily utilizes the rain garden's storage layer to retain rainwater but does not consider the rain garden's infiltration capacity or void water storage capacity. The proportional estimation method based on the catchment area generally recommends an area of 5% to 10% of the catchment area, but it

lacks precision. Xiang Lulu et al. proposed a more precise complete water balance method by comprehensively considering the water storage capacity and soil permeability of rain gardens. The formula for calculating the surface area of a rain garden is shown in Equation (1).

$$A_f = \frac{A_d H \varphi d_f}{60 \times KT(d_f + h) + h_m(1 - f_v)d_f + nd_f^2} \tag{1}$$

where A_f —rainwater garden area, m^2, A_d —catchment area, m^2, H —design rainfall, m, φ —runoff coefficient, d_f — depth of the rain garden, m, K — soil permeability coefficient, m/s, T — calculation period, $\min$, typically 15 minutes for a short-duration rainfall event, h —Design average water depth of the storage layer, m, h_m —Maximum storage height, m, f_v —Percentage of plant cross-sectional area relative to the storage layer surface area, typically 15%, n —Average porosity of the planting soil and fill material layer, typically around 0.4.

II. B.SWMM Modeling Principles

For the SWMM model, sub-catchment areas are the smallest independent units used for simulation calculations. They can be used to simulate and analyze the impact of surface changes on hydrological processes under different surface conditions. The structure of the SWMM model is shown in Figure 1.

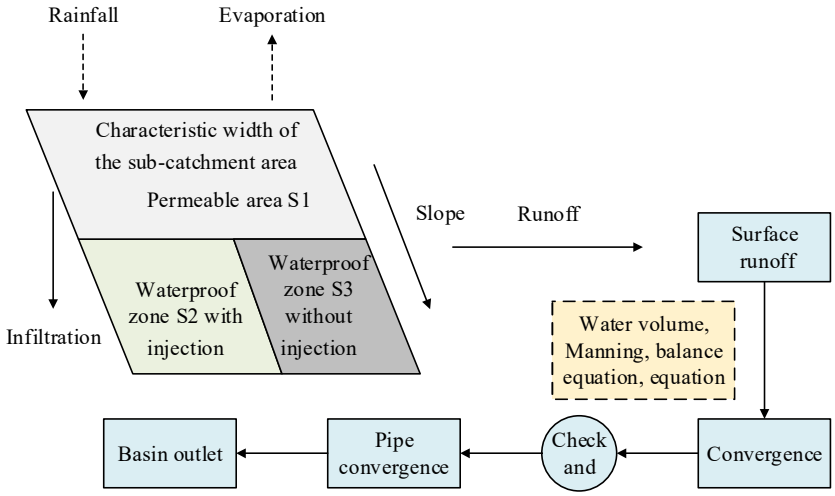

Figure 1: Structure of the SWMM model

(1) Principles of Surface Runoff Calculation

Surface runoff refers to the process by which rainfall in a given area becomes net rainfall after accounting for losses due to soil infiltration, evaporation, vegetation interception, and depression storage. When using the SWMM model to simulate hydrological processes in the study area, it is necessary to first divide the study area into sub-catchment zones. According to the model principles, sub-catchment zones can be divided into permeable and impermeable areas. Where the impermeable area further includes two parts: the impermeable area with depressions S_2 and the impermeable area without depressions S_3. The division results are shown in Figure 2. When simulating the urban rainfall-runoff process, the runoff processes of each sub-catchment area are independent of each other. The sub-catchment area is divided into three sub-regions, each of which undergoes separate runoff calculations. The final runoff volume for each sub-catchment area is determined by summing the runoff volumes of the permeable and impermeable regions, i.e., the sub-catchment area runoff volume equals the sum of the permeable and impermeable region runoff volumes.

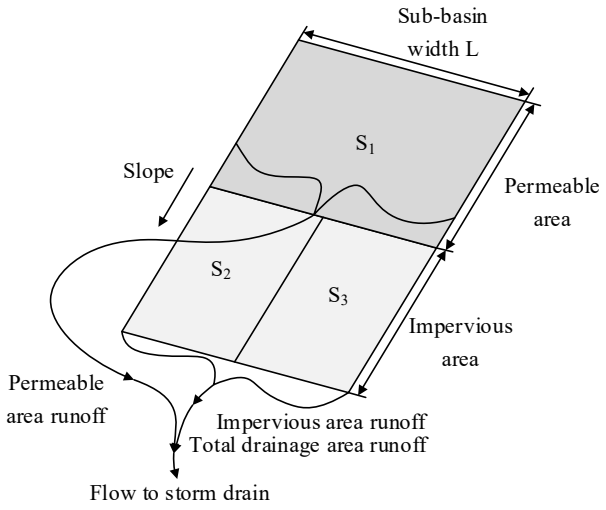

Figure 2: Flow generation process in Sub-catchment area

1) Permeable zone (S_1) production flow rate, expressed as:

$$R_1 = (i - f) \cdot \Delta t \tag{2}$$

In the formula:

R_1 —permeable zone yield, mm;

i —rainfall intensity, mm/s;

f —infiltration intensity, mm/s.

2) Yield of impermeable zone (S_2) with depressions, yield is expressed as:

$$R_2 = P - D \tag{3}$$

In the formula:

R_2 —flow rate in the impermeable area with depressions, mm;

P —rainfall, mm;

D —depression storage capacity, mm.

3) Flow rate in the impermeable area without depressions (S_3), expressed as:

$$R_3 = P - E \tag{4}$$

In the formula:

R_3 —flow rate in the impermeable area without depressions, mm;

P —rainfall, mm;

E —evaporation, mm.

(2) Principle of calculating infiltration water volume

Infiltration refers to the process by which precipitation seeps through the ground surface into permeable zones. The SWMM model includes the Horton, Green-Ampt, runoff curve, and three different types of infiltration models to simulate runoff in permeable zones.

1) Horton Model

During rainfall, the infiltration rate of rainwater in unsaturated soil decreases from a maximum value to a stable rate. Based on this change pattern, the Horton model was proposed. This model does not consider the relationship between the saturated and unsaturated zones of the soil, so the Horton model was selected for infiltration rate calculations in this study. In this model, the key parameters are the maximum and minimum infiltration rates. The principle formula of the Horton model can be expressed as:

$$f_p = f_\infty + (f_0 - f_\infty) e^{-kt} \tag{5}$$

In the equation:

f_p —soil infiltration rate (mm/h);

f_0 —initial infiltration rate (mm/h);

f_∞ —steady-state infiltration rate (mm/h);

k —infiltration decay coefficient $(1/h)$;

t —infiltration duration (h).

2) Green-Ampt model

The Green-Ampt model assumes the existence of two layers, namely the initial soil water table and the saturated soil water table. The boundary line between the two layers is called the wet front. An example of the model division is shown in Figure 3, and the mathematical principle formula is shown in (6):

$$F = \frac{K_s S_w (\theta_s - \theta_i)}{i - K_s} \tag{6}$$

In the equation:

θ_s —saturated water content;

θ_i —initial water content;

S_w —water absorption capacity of soil at the wetting front;

i —rainfall intensity (mm);

K_s —permeability coefficient of saturated soil.

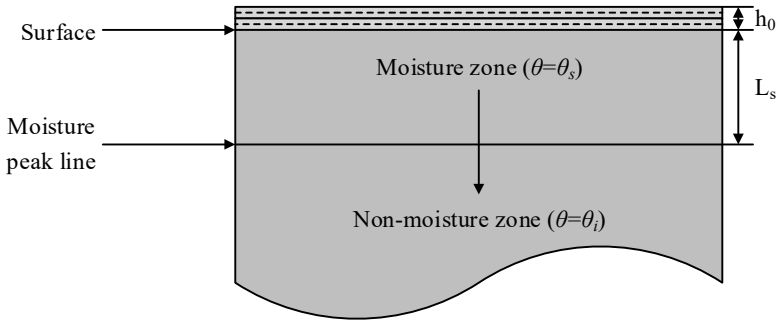

Figure 3: Example of Green-AMPT percolation model

3) SCS-CN model

There is a correlation between the water storage capacity of soil and the curve number (CN), and the SCS-CN model was proposed based on this correlation. The specific calculation formula is as follows:

$$PE = \frac{(P - I_a)^2}{(P - I_a + S)} \tag{7}$$

In the formula:

I_a —initial loss;

P —cumulative rainfall;

PE —cumulative effective rainfall;

S —potential maximum storage capacity

(3) Surface runoff calculation principle

When studying surface runoff in a watershed, the SWMM model uses nonlinear reservoir theory to simulate surface runoff in sub-basins with three characteristics. The model comprehensively considers key parameters such as the surface area of the sub-basin, ground slope, and rainfall intensity, and uses a combination of Manning's formula and the water balance equation to calculate the surface runoff process.

The simulation calculation formula is as follows:

$$\frac{dV}{dt} = A\frac{dh}{dt} = Ai - Q \tag{8}$$

$$Q = 1.49 \times \frac{W}{n}(h - h_p)^{\frac{5}{3}} S^{\frac{1}{2}} \tag{9}$$

In the equation:

h —water depth, m;

t —time, s;

A —sub-drainage area, m^2;

i —net rainfall intensity, mm/s;

Q —flow rate, m^3/s;

W —sub-catchment area width, m;
n —Manning's roughness coefficient;
h_p —storage depth, m;
S —sub-catchment area slope.

(4) Principles of Pipeline Convergence Calculation

Pipeline convergence refers to the process by which rainwater runoff flows into inspection wells, enters the urban drainage network through the inspection wells, and ultimately exits the urban drainage network. Constant flow, moving wave, and dynamic wave are the three computational methods for water flow in pipelines.

1) Steady Flow

When calculating pipeline flow using the steady flow method, it is assumed that the flow rate remains constant and uniform throughout each calculation time interval. A simple equation is used to calculate the pipeline flow rate. The steady flow algorithm is only applicable to tree-shaped conveyance pipeline networks. This method cannot estimate backflow in pipelines, losses at inlets and outlets, reverse flow, or pressurized flow conditions, and is only effective for long-term continuous simulation analysis.

2) Moving Wave Method

The moving wave method reflects changes in channel flow and area over time and space. Its calculation method combines the continuity equation and the momentum equation to simulate the dynamic flow of water in drainage systems, ensuring numerical stability in calculations. The moving wave method has a high time step characteristic, but it has limitations in simulating channel backflow, inlet/outlet losses, reverse flow, and pressurized flow.

3) Dynamic wave

The dynamic wave method calculates flow convergence by solving the Saint-Venant equations, and can be used to simulate water depth at nodes in rainwater drainage systems and the movement of pressurized water flow within pipes. Compared to the other two methods, the dynamic wave method is applicable to all currently existing drainage systems and effectively addresses issues such as pressurized flow, backflow, and reverse flow. This method is the most accurate of the three, so it was selected for this study. The calculation formula is as follows.

$$\frac{\partial Q}{\partial x}+\frac{\partial A}{\partial t}=0 \tag{10}$$

$$\frac{\partial H}{\partial x}+\frac{v}{g}\frac{\partial v}{\partial x}+\frac{1}{g}\frac{\partial v}{\partial t}=S_0-S_f \tag{11}$$

$$Q=\frac{1}{n}AR^{\frac{2}{3}}S_0^{\frac{1}{2}} \tag{12}$$

In the equation:

Q —outflow rate, m^3/s;
A —cross-sectional area, m^2;
v —velocity, m/s;
x —pipe length, m;
R —hydraulic radius, m;
H —water depth, m;
S_f —friction coefficient;
S_0 —gravity term;
g —gravitational acceleration, taken as $9.8m/s^2$;
n —Manning coefficient.

III. Case study of the hydrological effects of smart technology in urban rain garden design

III. A. Overview of the Study Area

III. A. 1) Geographic location

City A is located at 40°21' to 41°45' north latitude and 120°78' to 122°99' east longitude, in the northern part of Province X, China. The study area is an administrative region established alongside the development of City A and serves as the city's main urban district. As the political, economic, educational, cultural, and transportation hub of City A, the study area has been awarded numerous honors, including the titles of National Water-Saving City and National Hygienic City.

III. A. 2) Climate Conditions

The study area is rich in solar and thermal resources and has a warm temperate monsoon climate, characterized by mild temperatures and distinct seasons. Southeast winds prevail in spring and summer, while northeast winds dominate in autumn and winter. Spring temperatures are variable, summers are hot, winters are cold, and autumns are clear and pleasant. The annual average temperature is $15.2^{\circ}C$. Precipitation is significantly influenced by the monsoon climate, with little interannual variation but uneven distribution within the year. Spring is prone to drought, summer to flooding, and autumn and winter to dryness. The long-term average precipitation is approximately $905.3mm$.

According to meteorological data from A City over the past 20 years: the annual average temperature shows an upward trend, with a minimum of $12.1^{\circ}C$ and a maximum of $16.2^{\circ}C$; wind speed and sunshine duration show a decreasing trend year by year; Annual precipitation shows an upward trend, with precipitation levels in 2000, 2002, and 2003 reaching 1,301.5 mm, 1,399.2 mm, and 1,295.4 mm, respectively. Summer precipitation shows a significant increase, while autumn precipitation shows a decrease.

III. A. 3) Hydrological landforms

The terrain within City A is highly undulating, with a general northwest-high, southeast-low configuration. Most areas have an altitude below 50 meters, with the highest and lowest altitudes being 69.4 meters and 3.3 meters, respectively. City A has a dense network of rivers, with numerous main flood control channels that discharge approximately $18km^2$ of floodwater from the middle and upper reaches.

III. A. 4) Land Types

The specific values for the proportion of land use types in the study area are shown in Table 1. The land use types in the study area exhibit obvious urbanization characteristics, with highways having the highest imperviousness rate (85%) and accounting for 12.22% of the total area, which has a significant impact on regional runoff.

Table 1: Proportion of Land Use Types in Area

Serial number	Land use type	Impermeable water/%	Area/ha	Area proportion/%
1	Park	28	40.79	13.16
2	Government building	55	15.58	5.03
3	Square	70	15.17	4.89
4	Building area	78	100.51	32.42
5	Construction area	79	50.97	16.44
6	Grassland	5	37.33	12.04
7	River channel	-	8.67	2.80
8	Scenic Lake	2	3.11	1.00
9	Highway	85	37.87	12.22
Total	-	-	310	100

III. B. Research on the Hydrological and Environmental Effects of Rainwater Gardens

To investigate the hydrological characteristics of LID facilities in the study area and the differences in hydrological performance outcomes resulting from different drainage methods, a paired experimental monitoring approach was proposed based on rainfall data from the study area. This involved constructing two parallel rain gardens in an area with shallow groundwater levels, one equipped with a drainage system (drainage type) and the other without (infiltration type). The aim was to provide data support for the rational implementation of sponge city construction in the study area, achieving the objectives of rainwater "storage, retention, purification, utilization, and discharge" of rainwater in the study area.

III. B. 1) Hydrological effects

The runoff process of infiltration-type rain gardens (RG-inf) includes inflow and outflow processes. The runoff process of drainage-type rain gardens (RG-dr) is divided into three parts: inflow, outflow, and drainage. Following urbanization, natural ground surfaces have gradually been replaced by hardened pavements, gray buildings, and other structures, obstructing the natural infiltration of rainfall runoff. As a result, the convergence time of rainfall runoff during heavy rains has significantly shortened, peak runoff occurs earlier, and runoff volume has doubled, remaining stagnant on hardened surfaces, thereby exacerbating flood and waterlogging issues. The rainfall runoff processes before and after urbanization are shown in Figure 4. It can be seen that after development, the flood

peak is larger and occurs earlier. The development of LID technologies such as rain gardens aims to make the hydrological conditions of the developed area as consistent as possible with those before development.

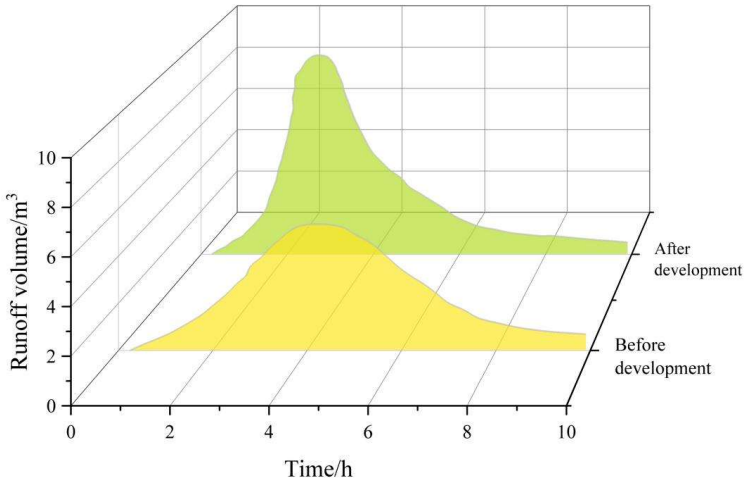

Figure 4: The process of rainstorm runoff before and after urbanization

The results of the calculation of inflow, outflow, and peak lag time for representative rainfall events are shown in Table 2. The selected time period is June–July 2024, which includes one complete rainy season rainfall monitoring process. Among the 8 rainfall events, the average peak retention time for RG-inf was 89.125 minutes, while the corresponding value for RG-dr was 34.125 minutes, indicating that the drainage-type design has a significant advantage in flood peak regulation. During the July 31 rainfall event, RG-inf achieved 100% peak reduction, while RG-dr achieved 96.5%. However, during heavy rainfall events, the peak reduction rate of RG-inf was significantly lower than that of RG-dr, indicating that the drainage-type design has stronger adaptability to heavy rainfall.

Table 2: Calculation results of inflow and outflow Rates and peak stay time

Time	Rainfall /mm	Rainfall category	RG-inf				RG-dr			
			Inflow rate /m^3	Drainage volume /m^3	Peak lag time /min	Peak reduction rate /%	Inflow rate /m^3	Drainage volume /m^3	Peak lag time /min	Peak reduction rate /%
6.1	29.4	Heavy rain	6.11	2.98	68	40.2	6.37	2.74	2	99.4
6.10	16.8	Moderate rain	3.12	0.66	46	61.8	2.64	1.48	75	98.3
6.20	9.2	Moderate rain	1.03	0.14	97	83.6	1.15	0.33	98	93.4
6.30	18.5	Moderate rain	1.77	0.75	25	71.4	2.26	0.89	6	96.9
7.1	30.1	Heavy rain	4.37	2.77	155	22.7	4.85	2.75	4	98.1
7.10	10.6	Moderate rain	1.54	0.32	35	78.9	1.64	1.34	53	80.2
7.20	8.5	Moderate rain	1.03	0.18	60	96.5	1.04	0.57	14	97.9
7.31	9.1	Moderate rain	0.82	0.00	227	100.0	0.83	0.51	21	96.5

Due to significant differences in rainfall intensity, duration, and the number of preceding sunny days, the inflow and outflow processes of each rainfall event vary greatly. Two typical rainfall events, Huff1 and Huff2, were selected, and their inflow and outflow processes are shown in Figure 5 (a–b). The inflow processes of both rain gardens are closely related to the rainfall intensity and the uniformity of rainfall distribution during the rainfall event. The peak values of the inflow flow rate also increase with increasing rainfall intensity. For each rainfall event, both the roof runoff and the runoff produced by the rain garden system exhibit the same peak and trough characteristics as the

rainfall duration progresses, until the rainfall ends. The real-time changes in rainfall intensity directly affect the size of the inflow volume. When the inflow volume exceeds the infiltration volume, standing water forms on the surface of the rain garden's storage layer. When the standing water exceeds the height of the outflow weir, the rainwater is discharged into the traditional urban stormwater drainage system, and the rain garden's storage process reaches a dynamic equilibrium. In the monitored rainfall events, for the two rain gardens where no overflow events occurred, the rainfall distribution range was between 0 and 7 mm, primarily consisting of light to moderate rain. For heavy rain and torrential rain events, the timing of inflow and outflow depends on the distribution of rainfall intensity, and the peaks of inflow and outflow also fluctuate with changes in rainfall intensity.

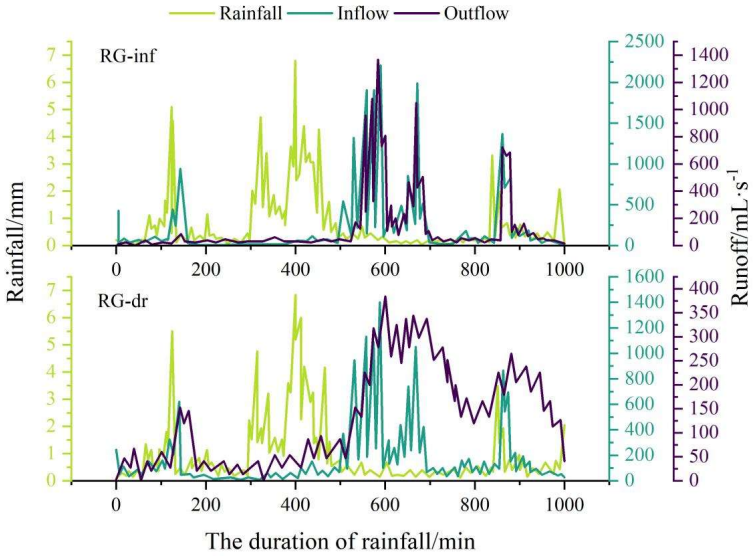

(a)Huff1

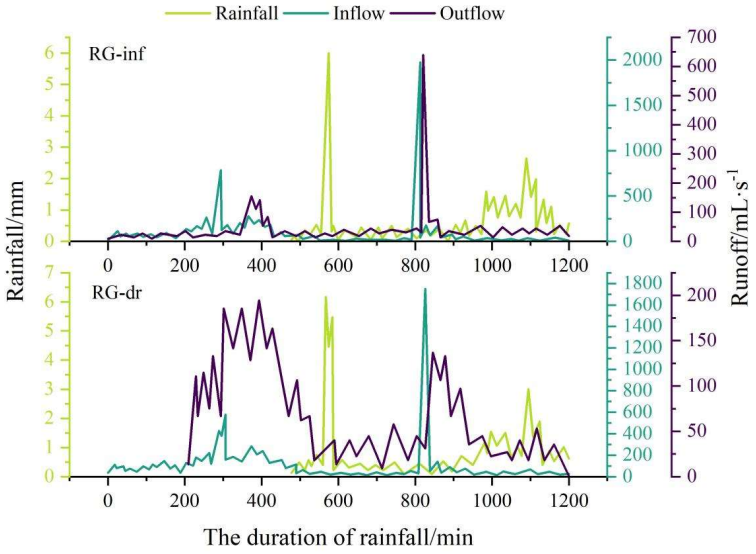

(b)Huff2

Figure 5: Typical rainfall inflow and outflow processes

III. B. 2) Hydraulic effects

The main outfall of the stormwater drainage system is typically located near natural water bodies. Analyzing it can provide scientific basis for urban flood control and drainage planning. The study area has three main outfalls, all connected to the municipal stormwater drainage system. Analyzing their flow and water depth can aid in pipeline load assessment and pipeline layout optimization. Here, we take the O1 main outfall (the outfall on the southern side of the study area) as an example for analysis. Under the RG-inf scenario, the water depth and flow analysis

results for the O1 main outfall under two typical rainfall patterns are shown in Figure 6 (a–b). The trends in flow and water depth at the main outfall generally align with the rainfall process line, and the water depth change process line is more gradual than the flow change process line. Under the Huff2 rainfall scenario, the peak flow is the smallest, at 0.25 m/s.

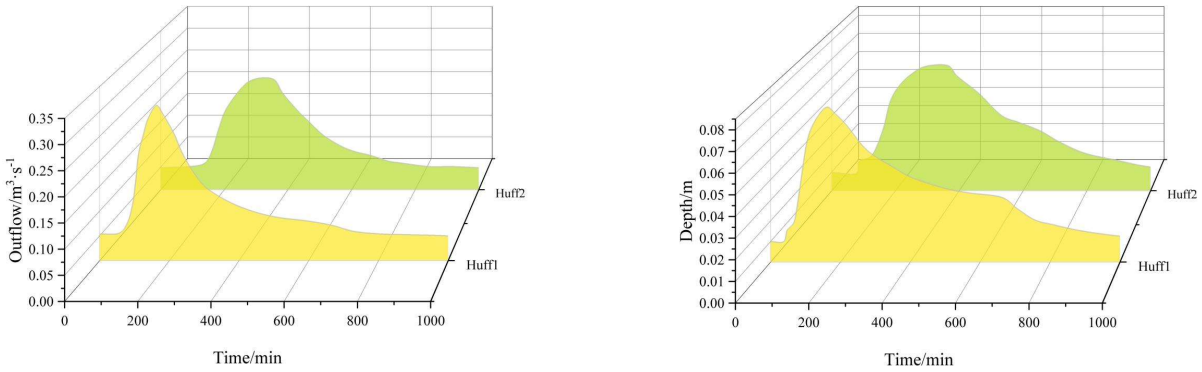

(a)Outflow (b)Depth

Figure 6: Results of water depth and outflow analysis

The results of the flow process analysis of the total discharge outlet O1 under two typical rainfall patterns are shown in Figure 7. In RG-dr, due to the small amount of rainfall, the water depth and peak flow time of the total discharge outlet changed less than in RG-inf, but the total flow and peak flow were significantly reduced. At the same time, the simulation results for the O2 and O3 total discharge outlets verified the above pattern.

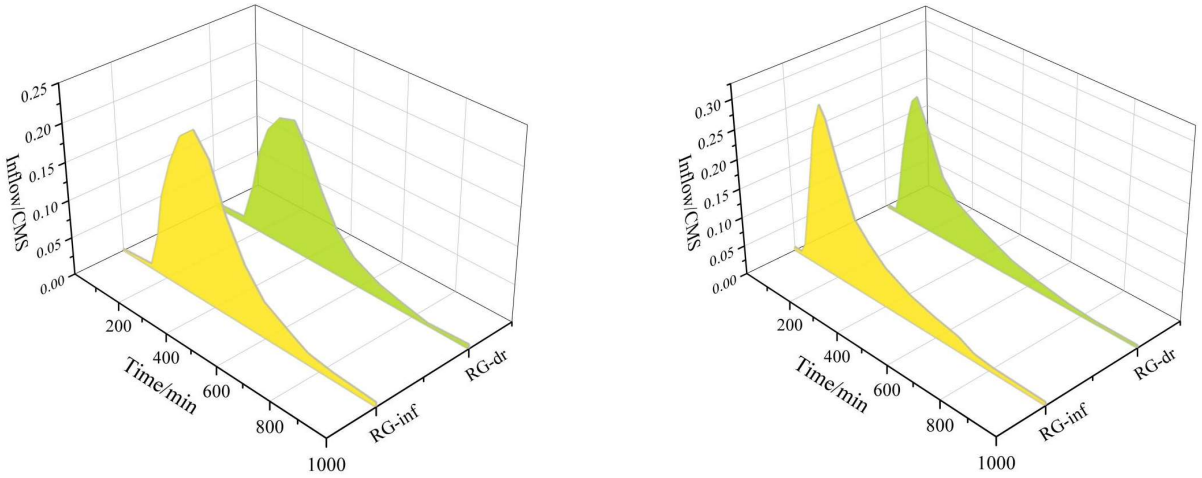

(a)Huff1 (b)Huff2

Figure 7: O1 Results of flow process analysis

III. B. 3) Environmental Effects

To assess the effectiveness of LID facilities in controlling runoff pollutants in the study area, four water quality indicators—SS, COD, TN, and TP—were selected as the research objects. The patterns of pollutant changes were analyzed, and the total pollutant loads for each runoff pollutant are shown in Table 3. The average total pollutant loads for the four categories of pollutants (SS, COD, TN, and TP) in RG-inf were 79.750 kg, 20.532 kg, 10.929 kg, and 1.484 kg, respectively, while those in RG-dr were 56.383 kg, 13.725 kg, 7.484 kg, and 0.904 kg, respectively. The average removal rates for the total loads of the four pollutants (SS, COD, TN, and TP) were 29.30%, 33.15%, 31.52%, and 39.08%, respectively. The results indicate that RG-dr has a good regulatory effect on non-point source pollution. On the one hand, RG-dr controls the total runoff volume while removing part of the pollutants. On the

other hand, RG-dr controls the total pollutant load of runoff through functions such as sedimentation, filtration, and adsorption.

Table 3: Total pollutant load of each runoff

Water quality indicators	Development mode	Total load/kg		
		Huff1	Huff2	Mean value
SS	RG-inf	79.386	80.114	79.750
	RG-dr	56.228	56.538	56.383
COD	RG-inf	20.486	20.578	20.532
	RG-dr	13.554	13.896	13.725
TN	RG-inf	10.772	11.086	10.929
	RG-dr	7.337	7.631	7.484
TP	RG-inf	1.462	1.506	1.484
	RG-dr	0.895	0.913	0.904

III. C. Landscape Effect Analysis

III. C. 1) User Preference Analysis

This paper surveyed the preferences of 207 users of different age groups, and the results of the preference analysis are shown in Figure 8. Most users considered the landscape effect of RG-dr to be relatively good, with more than 50% of users in all age groups rating it as “very good” or “good.” Users' preference for the landscape effect of RG-inf was relatively poor, with more than 20% of users giving it a poor rating.

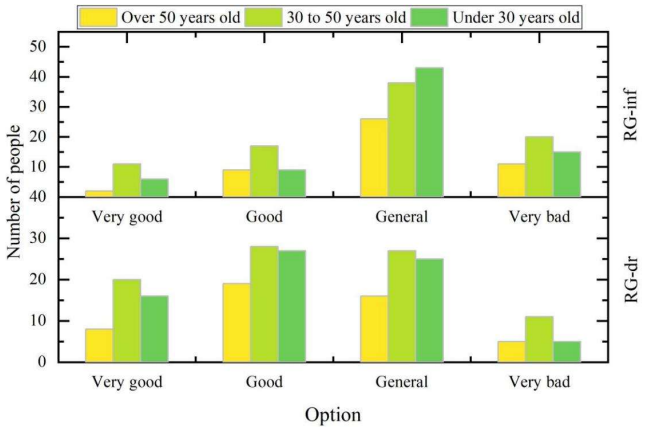

Figure 8: Preference analysis results

III. C. 2) Landscape Hierarchy Analysis

The results of the RG-inf and RG-dr landscape hierarchy analysis are shown in Figure 9. Users generally believe that the RG-dr landscape hierarchy is more rich, with more than 60% of users of all age groups evaluating it as “very rich” or “relatively rich.”

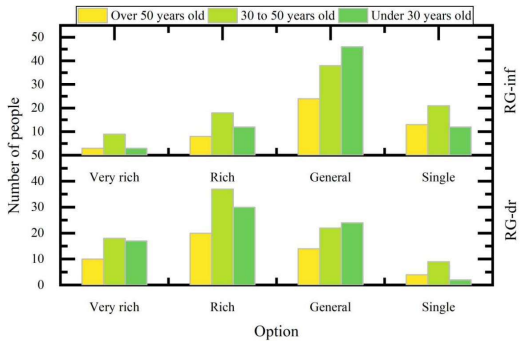

Figure 9: Landscape hierarchy analysis results

IV. Conclusion

This study combined the SWMM model with field monitoring to confirm that smart technology can optimize the hydrological performance and environmental benefits of rain gardens. The main conclusions are as follows.

(1) In eight rainfall events, the average peak retention time of RG-inf was 89.125 minutes, while that of RG-dr was 34.125 minutes. During the July 31 rainfall event, RG-inf achieved 100% peak reduction, while RG-dr achieved 96.5%. However, during heavy rainfall events, the peak reduction rate of RG-inf was significantly lower than that of RG-dr, indicating that drainage-type designs have stronger adaptability to heavy rainfall.

(2) In RG-dr, due to the smaller rainfall volume, the changes in total outlet water depth and peak flow occurrence time were smaller than those in RG-inf, but the total flow and peak flow reduction were significant. The average total loads of the four types of pollutants in RG-dr were 56.383 kg, 13.725 kg, 7.484 kg, and 0.904 kg, respectively. The average removal rates for the total pollutant loads of SS, COD, TN, and TP were 29.30%, 33.15%, 31.52%, and 39.08%, respectively.

(3) In terms of landscape benefits, most users considered the landscape effect of RG-dr to be relatively good, with over 50% of users of all age groups rating it as “very good” or “good.” Users' preference for the landscape effect of RG-inf was relatively poor, with over 20% of users giving it a negative rating. Users generally considered the landscape layers of RG-dr to be relatively rich, with over 60% of users of all age groups rating it as “very rich” or “relatively rich.”

Acknowledgements

This paper was supported by the research project of Fuzhou Science and Technology Association in 2024, "Suggestions on Improving the resilience prevention and control system of flood control and drainage in Fuzhou Urban Area".

References

[1] Liu, Y., Zhao, W., Wei, Y., Sebastian, F. S. M., & Wang, M. (2023). Urban waterlogging control: A novel method to urban drainage pipes reconstruction, systematic and automated. Journal of Cleaner Production, 418, 137950.

[2] Kriech, A. J., & Osborn, L. V. (2022). Review of the impact of stormwater and leaching from pavements on the environment. Journal of Environmental Management, 319, 115687.

[3] Bai, T., Mayer, A. L., Shuster, W. D., & Tian, G. (2018). The hydrologic role of urban green space in mitigating flooding (Luohe, China). Sustainability, 10(10), 3584.

[4] Chen, S. S., Kimirei, I. A., Yu, C., Shen, Q., & Gao, Q. (2022). Assessment of urban river water pollution with urbanization in East Africa. Environmental Science and Pollution Research, 29(27), 40812-40825.

[5] Wu, P., Zhong, K., Wang, L., Xu, J., Liang, Y., Hu, H., ... & Le, J. (2022). Influence of underlying surface change caused by urban renewal on land surface temperatures in Central Guangzhou. Building and Environment, 215, 108985.

[6] Pan, Y., Li, Z., Gao, Y., Xiong, Y., Qiao, Y., Tao, Y., ... & Zang, C. (2021). Analysis of the migration characteristics of stormwater runoff pollutants on different underlying surfaces in Guangzhou, China. Frontiers in earth science, 9, 554588.

[7] Gao, H., Cai, H., & Duan, Z. (2018). Understanding the impacts of catchment characteristics on the shape of the storage capacity curve and its influence on flood flows. Hydrology Research, 49(1), 90-106.

[8] Alshammari, E., Rahman, A. A., Rainis, R., Seri, N. A., & Fuzi, N. F. A. (2023). The impacts of land use changes in urban hydrology, runoff and flooding: a review. Current Urban Studies, 11(1), 120-141.

[9] Zhao, L., Zhang, T., Li, J., Zhang, L., & Feng, P. (2023). Numerical simulation study of urban hydrological effects under low impact development with a physical experimental basis. Journal of Hydrology, 618, 129191.

[10] Nguyen, T. T., Ngo, H. H., Guo, W., Wang, X. C., Ren, N., Li, G., ... & Liang, H. (2019). Implementation of a specific urban water management-Sponge City. Science of the Total Environment, 652, 147-162.

[11] Sharma, R., & Malaviya, P. (2021). Management of stormwater pollution using green infrastructure: The role of rain gardens. Wiley Interdisciplinary Reviews: Water, 8(2), e1507.

[12] Chen, C., Li, Y., Le, W., You, C., Liu, Z., Liu, W., & Zhang, R. (2023). Field performance of rain garden in red soil area in southern China. Water, 15(2), 267.

[13] Wanitchayapaisit, C., Suppakittpaisarn, P., Charoenlertthanakit, N., Surinseng, V., Yaipimol, E., & Rinchumphu, D. (2022). Rain garden design for stormwater management in Chiang Mai, Thailand: A Research-through-Design Study. Nakhara: Journal of Environmental Design and Planning, 21(3), 222-222.

[14] Liu, W., Pei, Q., Dong, W., & Chen, P. (2022). Study on the purification capacity of rain garden paving structures for rainfall runoff pollutants. Archives of Environmental Protection, 28-36.

[15] Jacque, H., Knox, J. W., Gush, M., & Holman, I. P. (2023). Modelling the potential of rainwater harvesting to improve the sustainability of landscape and public garden irrigation. Journal of Environmental Management, 348, 119167.

[16] Burszta-Adamiak, E., Biniak-Pieróg, M., Dąbek, P. B., & Sternik, A. (2023). Rain garden hydrological performance–Responses to real rainfall events. Science of the Total Environment, 887, 164153.

[17] Zhou, Z., & Guo, Q. (2022). Drainage alternatives for rain gardens on subsoil of low permeability: Balance among ponding time, soil moisture, and runoff reduction. Journal of Sustainable Water in the Built Environment, 8(3), 05022002.

[18] Zhang, L., Oyake, Y., Morimoto, Y., Niwa, H., & Shibata, S. (2019). Rainwater storage/infiltration function of rain gardens for management of urban storm runoff in Japan. Landscape and Ecological Engineering, 15, 421-435.

[19] Riley, E. D., Kraus, H. T., Bilderback, T. E., Owen Jr, J. S., & Hunt, W. F. (2018). Impact of engineered filter bed substrate composition and plants on stormwater remediation within a rain garden system. Journal of Environmental Horticulture, 36(1), 30-44.

[20] Alyaseri, I., Zhou, J., Morgan, S. M., & Bartlett, A. (2017). Initial impacts of rain gardens' application on water quality and quantity in combined sewer: Field-scale experiment. Frontiers of Environmental Science & Engineering, 11, 1-12.
[21] Zhang, L., Ye, Z., & Shibata, S. (2020). Assessment of rain garden effects for the management of urban storm runoff in Japan. Sustainability, 12(23), 9982.
[22] Kravchenko, M., Tkachenko, T., Mileikovskyi, V., & Trach, Y. (2024). Quantitative assessment of hydrological efficiency of rain garden design in the context of managing the volume and quality of storm effluent. Acta Scientiarum Polonorum. Architectura, 23, 369-383.
[23] Kravchenko, M., Wrzesiński, G., Pawluk, K., Lendo-Siwicka, M., Markiewicz, A., Tkachenko, T., ... & Piechowicz, K. (2024). Improving Urban Stormwater Management Using the Hydrological Model of Water Infiltration by Rain Gardens Considering the Water Column. Water, 16(16), 2339.
[24] Jia, X. L., Yang, Q., Liang, H., Qi, X. P., & Rong, X. W. (2025). Prediction of rain garden runoff control effects based on multiple machine learning techniques. Environmental Technology, 1-12.
[25] Jeon, M., Guerra, H. B., Choi, H., Kwon, D., Kim, H., & Kim, L. H. (2021). Stormwater runoff treatment using rain garden: performance monitoring and development of deep learning-based water quality prediction models. Water, 13(24), 3488.
[26] Kumar, S., & Singh, K. K. (2021). Rain garden infiltration rate modeling using gradient boosting machine and deep learning techniques. Water Science and Technology, 84(9), 2366-2379.
[27] Zhao, Y., Zeng, W., Ni, Y., Xia, P., & Tan, R. (2023, November). Research and Design of Hydrological Data Visualization Based on Digital Twin. In International Artificial Intelligence Conference (pp. 277-289). Singapore: Springer Nature Singapore.
[28] Villalba, G., Plaza, F., Zhong, X., Davis, T. W., Navarro, M., Li, Y., ... & Liang, X. (2017). A networked sensor system for the analysis of plot-scale hydrology. Sensors, 17(3), 636.